Study of constant current and ripple current aging of LT-PEMFC stacks

Gautier Capdeville, Amine Jaafar, Fabien Lacressonnière, Christophe Turpin, Thomas Jarry, Emilie Soyez, Pierre Henrard, Paul Kreczanik, André Rakotondrainibe, Manuel Espinosa, Benoit Guenot

***Abstract*— In order to minimize fuel cell aging, it is important to take into account the interactions of fuel cells with the auxiliaries required for their operation. In particular, in this study, we focus on the impact of current harmonics generated by the static converter connected to a Low Temperature Proton Exchange Membrane Fuel Cell (LT-PEMFC) technology stack. Indeed, today, there are still uncertainties about the influence of current harmonics on the acceleration of fuel cell aging, especially following technological developments tending to reduce the membrane thickness. In this paper, two endurance tests are carried out simultaneously on two test benches to compare the aging of an LT-PEMFC stack operating in the presence of current harmonics emulating the presence of a Boost DC-DC converter with a stack of the same technology operating at the same constant average current. The results obtained are analyzed and compared on the basis of voltage degradation rates observed during endurance and those recorded via polarization curves. The work presented in this study was carried out as part of the HEMOWHY (HEavy MObilities With HYdrogen) project.**

Keywords*— *Hydrogen, Fuel cell, LT-PEMFC, Stack, Aging, Current harmonics, Power converter.

I. INTRODUCTION

New electric mobility solutions based on fuel cells (FC) are emerging against climate change. The lifetime of these FCs is a critical issue for their commercialization, and the challenges of durability and performance are crucial [1- 3]. In order to increase their lifetime, it is essential to take into account the interactions of FCs with all the auxiliaries that ensure their operation, such as the air compressor, gas humidifiers, hydrogen recirculator and static converter [4-9].

In fact, the electrical energy produced by the FC is generally transmitted to the load via a static converter, which imposes current ripples on the FC current, whose frequency and amplitude are determined by converter's topology and control strategy [10]. The most common topologies of converters connected to a FC are Boost, Buck and inverter. FCs are often connected to a DC-DC Boost converter at the output to raise the voltage and/or a DC-AC inverter to convert DC to AC. Both of these converters impose high-frequency current harmonics (a few kHz to 100 kHz) on the load, but the inverter also has a low-frequency component at 100-120 Hz, and the impact of this component on FC aging needs to be studied further. A study has shown that a current ripple frequency of 100 Hz causes a greater and more visible decrease in performance on a PEM-FC after 100 hours of aging compared to frequencies of 1 kHz and 100 kHz [11]. But this paper will focus on the impact of high-frequency current harmonics such as those generated by a Boost converter on FC accelerated aging. Today, the impact of these harmonics on accelerated aging has not been fully confirmed in the literature. This needs to be further investigated, especially in the light of recent technological developments aimed at reducing the membrane thickness in order to minimize ohmic losses.

Several studies carried out at the Laplace lab [9], [10] have demonstrated the ability of the double-layer capacitor of a Low Temperature Proton Exchange Membrane fuel cell (LT-PEMFC) to filter HF current harmonics. The authors in [9] thus have shown that a frequency of 10 kHz is completely filtered out by the double-layer capacitor. Then the connection between a LT-PEM stack and a Boost converter was investigated and the results have highlighted the fact that the resulting amplitude of the stack voltage was not very high (1.2 %) whereas the impact on amplitude was greater in the case of connection with a Buck converter (6 %). So the authors have suggested adding a decoupling capacitor to limit the impact on the amplitude but in the case of a connection with a Boost converter, no current ripples filtering was recommended. Other scientific studies have shown an accentuation of FC aging under the effect of HF current harmonics [12], [13], while the authors of [14] are mixed and those of [15] have not noted any significant impact. New experimental tests need to be carried out using several cells or stacks in order to obtain a greater statistical effect, to enable the investigation of several frequencies of current ripples and to carry out longer aging campaigns. The results obtained should enable the power electronics engineer to design specifications for the design of a power converter that minimizes FC degradation and/or provide filtering of current ripples [16-18]. It is also important to take into account that

Gautier Capdeville (PhD student) is with the IRT Saint Exupéry, CS34436, 3 Rue Tarfaya, 31400 Toulouse. He is working at Laplace laboratory, LAPLACE, CNRS, Toulouse INP, Comue de Toulouse; 2 rue Charles Camichel, BP 7122, 31071 Toulouse (phone number : 0033788203944 and e-mails : capdeville@laplace.univ-tlse.fr, gautier.capdeville@irt-saintexupery.com).

Christophe Turpin, Amine Jaafar, Fabien Lacressoniere, Thomas Jarry and Emilie Soyez, LAPLACE, CNRS, Toulouse INP, Comue de Toulouse; 2 rue Charles Camichel, BP 7122, 31071 Toulouse (respective e-mails : turpin@laplace.univ-tlse.fr, jaafar@laplace.univ-tlse.fr, fablac@laplace.univ-tlse.fr, jarry@laplace.univ-tlse.fr, soyez@laplace.univ-tlse.fr).

Pierre Henrard, Paul Kreczanik are with IRT Saint Exupéry, CS34436, 3 Rue Tarfaya, 31400 Toulouse (respective e-mails : pierre.henrard@irt-saintexupery.com, paul.kreczanik@irt-saintexupery.com).

André Rakotondrainibe, Manuel Spinosa and Benoit Guenot are with ALSTOM Hydrogène SAS, 80 impasse Jean-Pierre Tennevin, 13290 Aix-en-Provence, France (respective e-mails : andre.rako@alstomgroup.com manuel.espinosa@alstomgroup.com, benoit.guenot@alstomgroup.com)

the switching frequency of power converters tends to be increased in order to reduce the size of the associated filters.

In this paper, the results of constant-current and ripple-current aging tests carried out on LT-PEM technology stacks will be analyzed and compared. Daily stop/start tests were carried out on each stack to limit the effect of reversible phenomena. Indeed, the aging of a FC can be made up of so-called irreversible losses linked to the intrinsic degradation mechanisms of its various components, and so-called reversible losses, mainly linked to the accumulation of water at the electrodes. To study the impact of HF current harmonics on the stacks aging, it is necessary to be able to distinguish between these two types of losses. Reversible losses can be more or less eliminated by the implementation of recovery processes (e.g. stop/start) [19]. This phenomenon of reversible losses tends to be accentuated by current ripples compared to a constant current. One hypothesis formulated in the literature is that HF current harmonics could favor the filling of activation layer nanopores with water [13], leading to long and deep FC flooding and thus to mechanical stress on the electrodes.

This study will focus on the aging generated by a constant current compared to that generated by a sinusoidal current ripple with a frequency of 10 kHz and a peak-to-peak amplitude of 20 % of the average current. The sinusoidal waveform was chosen because it is considered representative of the first harmonic of a realistic signal (triangular) emitted by a Boost converter. The sinusoidal waveform corresponds to the most energetic frequency harmonic which has potentially the greatest impact on FC aging.

The characterization tools used to monitor FC aging must not only serve to detect a drop in performance, but also to identify the underlying aging mechanisms and the conditions leading to their appearance. A review of the various diagnosis tools is given in [20]. These include polarization curves (V(I)), Electrochemical Impedance Spectroscopy (EIS) and Cyclic Voltammetry (CV). These techniques are also used to identify the parameters of quasi-static and dynamic models, providing a better understanding of the distribution of electrochemical losses within the FC [21]. By monitoring these parameters throughout the FC lifetime, it is possible to detect and predict the signature of certain degradation mechanisms. Prognosis methods have also been developed to estimate the state of health (SOH) of a FC and its remaining lifetime [22- 32]. In this way, it remains possible to control the FC operating conditions or the dynamics and level of the supplied current in order to preserve its SOH.

In this study, the section II presents a description of the used experimental test benches and the tested LT-PEM stacks. Next, the employed characterization tools will be explained and the operating conditions for the aging tests will be presented in section III. The results of the two aging tests will then be presented and compared in section IV. For reasons of confidentiality, the results are presented in per unit. Finally, a comparison of the evolution of degradation rates, obtained by two different methods during the aging tests, is carried out. The modeling of the impact of aging tests on stack performance is not covered in this paper and will be studied in a future work.

II. Description of Test Benches and Tested Stacks

A. Test benches

Aging tests under current ripples were carried out on two test benches at the Laplace laboratory's Hydrogen Platform (Fig. 1). These test benches are enable to run autonomously several sequences (start-up, stack characterization, shutdown) via a human-machine interface (HMI). This HMI is able to control all the fluidic and electrical components of the test benches.

B. Tested stacks

The tested stacks during these aging tests are some prototypes of a previous generation of LT-PEMFC technology supplied by ALSTOM Hydrogène. Theses stacks are formed with 5 cells. They can deliver a maximum electrical power of 1.5 kW. The membrane thickness of the stacks is in the range of [10;50] µm.

Just before starting the aging tests, each stack was activated for 24 h at a constant current recommended by the manufacturer (0.8 $A.cm^{-2}$). At the end of activation phase, the initial performance ($t = 0$) of the two stacks is obtained by plotting the polarization curves (Fig. 2). These represent the voltage evolution of the equivalent average cell (stack voltage divided by the number of cells) as a function of current density. Given the confidential aspect of some parts of this study, stack voltages and current densities are given in per unit.

In this work, the tested stack with a constant average current is named *Stack-I-Avg* whereas the one tested with a high-frequency current ripple is named *Stack-I-HF*.

III. Aging Test Procedure and Characterizations

Two aging tests are carried out in this study:

- *Stack-I-Avg* test: this is a constant-current cycling test (0.8 $A.cm^{-2}$) during 710 h. More precisely, the stack was only cycled for 655 h (with a current density of 0.8 $A.cm^{2}$), and the rest of the time was spent on characterizations and shutdowns phases, during which the stack was under nitrogen inert gas.
- *Stack-I-HF* test: it is a cycling test under sinusoidal current ripples of 10 kHz frequency, with an average value corresponding to 0.8 $A.cm^{-2}$ and a peak-to-peak amplitude equal to 20% of this average current density.

The duration of this test was 680 h, including 601 h of cycling (in the presence of current harmonics).

As mentioned in the introduction, daily stop/start operations are carried out to limit the impact of reversible phenomena. The various characterizations and operating conditions are described below.

A. *Characterization procedures*

During stacks aging tests, V(I) polarization curves were recorded on average once a week. These polarization curves are obtained in decreasing current steps from a maximal current density to OCV (Open Circuit Voltage). Each current step lasts 90 seconds, and the voltage measurement used for V(I) is the average of the voltages measured over the last 10 seconds of the step. After a stabilization time of 60 seconds per step, an EIS is performed, except for current steps below 0.2 A.cm^{-2}.

Figure 1: Test bench used for aging tests at the Laplace Hydrogen Platform

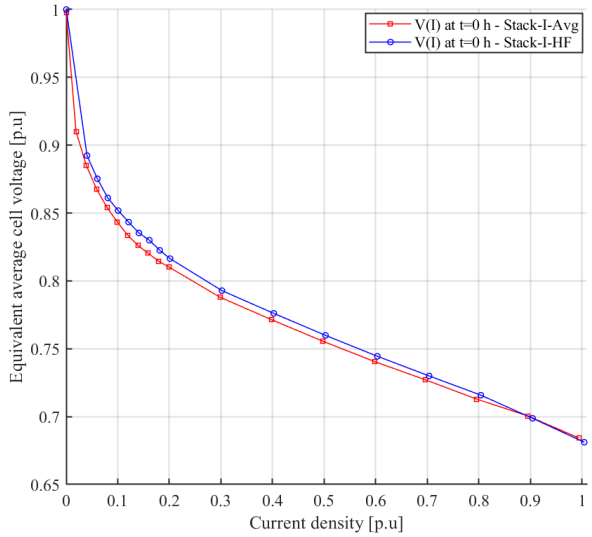

Figure 2: Initial polarization curves for both stacks with and without current harmonics

EIS is a characterization method that imposes a constant current on the FC, on which a sinusoidal excitation of variable frequency and low amplitude is superimposed, so as not to modify the FC behavior around this operating point.

Then for each excitation frequency, voltage and current are measured, and the component impedance is calculated and plotted in the Nyquist plane [33]. For the EIS performed during these tests, the peak-to-peak value of the sinusoidal excitation current is set at 2 A, and its frequency varies between 1 Hz and 20 kHz. Realized EIS allows measurement of the stack ohmic resistance and monitoring its variation as a function of current density. Variation of the ohmic resistance reflects the water state of the stack.

Some polarization curves are followed by cyclic voltammetry to quantify the influence of aging, particularly on the crossover current in the stack. This current reflects the deterioration of the membrane, resulting in internal leakage between the anode and cathode compartments. The cyclic voltammetries obtained and the crossover current measurements will be shown in the extended version of this paper.

An internal leakage test under inert gas (nitrogen) is also carried out after each polarization curve. This mechanical test assesses gas leakage between the anode and cathode compartments. An external leakage test is also carried out to ensure that the stack is leak-tight.

B. *Operating conditions for aging tests*

The two aging tests were carried out on two identical test benches under similar operating conditions. Operating conditions such as average stack temperature (T_{stack}), H_2 (P_{anode}) and air ($P_{cathode}$) pressures applied to the stack, relative humidities of H_2 (HR_{H2}) and air (HR_{AIR}) and overstoichiometry coefficients on the H_2 side (λ_{H2}) and on the air side (λ_{AIR}) are given in Table I.

IV. Aging Test Results

A. *Comparison based on the instantaneous evolution of the stack voltage*

The instantaneous voltage evolution of the equivalent average cell for the two aging tests is shown in Fig. 3. The *Stack-I-HF* test was stopped after 680 h, as the internal leakage rate threshold has been reached.

TABLE I. OPERATING CONDITIONS FOR AGING TESTS

Operating condition	Value
T_{stack} °C)	75
P_{anode} (bara)	2
HR_{H2} (%)	40
λ_{H2}	1.5
$P_{cathode}$ (bara)	2
HR_{AIR} (%)	40
λ_{AIR}	2

The evolution of these internal leakage rates as a function of test time is shown as a per unit in Fig. 4. Thus, from 450 h of testing for the *Stack-I-HF*, internal leakage rates increased significantly.

Fig. 3 also shows the voltage degradation rates between two consecutive characterizations. Degradation for the *Stack-I-HF* is relatively high at the start of the test (103 µV/h) compared with the *Stack-I-Avg* operating at constant current (77 µV/h). After this first week of testing, the degradation rates recorded for the *Stack-I-HF* are less pronounced than those observed for the *Stack-I-Avg*. It should also be noted that the constant current test is marked by a high recovery of reversible losses compared to the test with current harmonics.

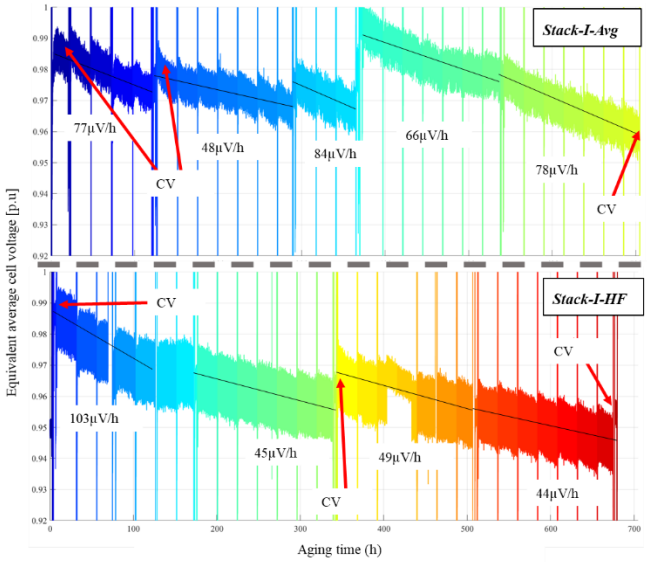

Figure 3: Evolution of the equivalent average cell voltage during the aging tests for the two stacks

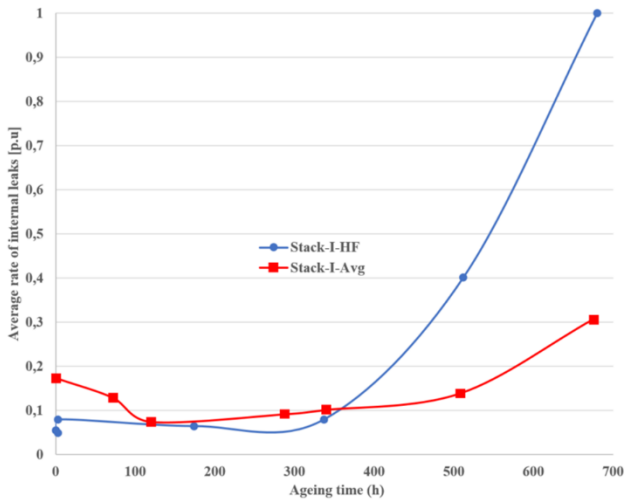

Figure 4: Internal leakage rates during aging tests

The characterization phases followed by cyclic voltammetry (CV) appear to have enabled better performance recovery for both stacks than a simple characterization phase with polarization curve and EIS only (Fig. 3).

B. Comparison based on the polarization curves

Fig. 5 shows the polarization curves at the beginning and the end of the aging tests for both stacks. The degradation rates obtained from polarization curves for two current densities (0.2 and 0.8 A.cm^{-2}) are summarized in Table II. These degradation rates correspond to the voltage drop at a given current density between the V(I) at time t and the initial V(I) (t =0 h), divided by the cumulative time of the aging test up to time t. This cumulative time takes into account only the time spent by the stack in cycling, and does not include characterization or shutdown phases. The results obtained show that the current harmonics test (*Stack-I-HF*) is about twice as degrading as the constant current test (*Stack-I-Avg*). Indeed, degradation rates for the *Stack-I-Avg* at 0.2 and 0.8 A.cm^{-2} are 11.98 and 21.77 µV/h respectively, whereas those for the *Stack-I-HF* are 25.1 and 42.15 µV/h for the same current densities and approximately the same test duration.

TABLE II. VOLTAGE DEGRADATION RATES DURING CYCLING FOR *BOTH STACKS AT TWO CURRENT DENSITIES OBTAINED FROM POLARIZATION CURVES*

Stack	V(I) considered in calculating degradation	Degradation rate at 0.2 A.cm^{-2} (µV/h)	Degradation rate at 0.8 A.cm^{-2} (µV/h)
Stack-I-Avg	V(I) at t = 710 h	11.98	21.77
Stack-I-HF	V(I) at t = 680 h	25.1	42.15

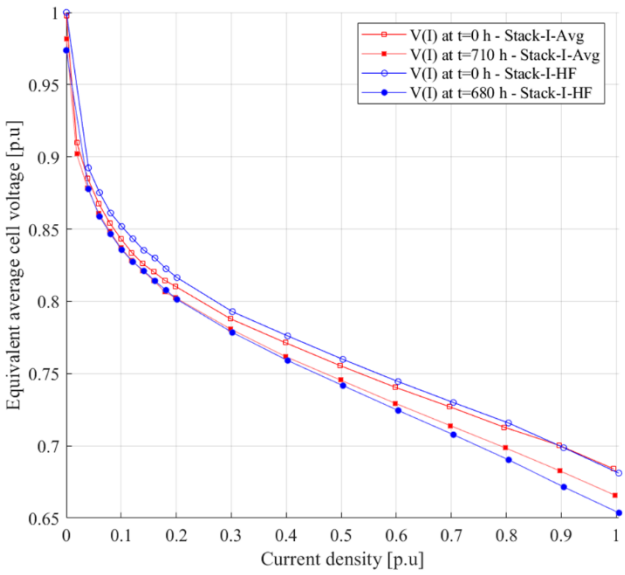

Fig. 5. Polarization curves for the two stacks at different times during current cycling.

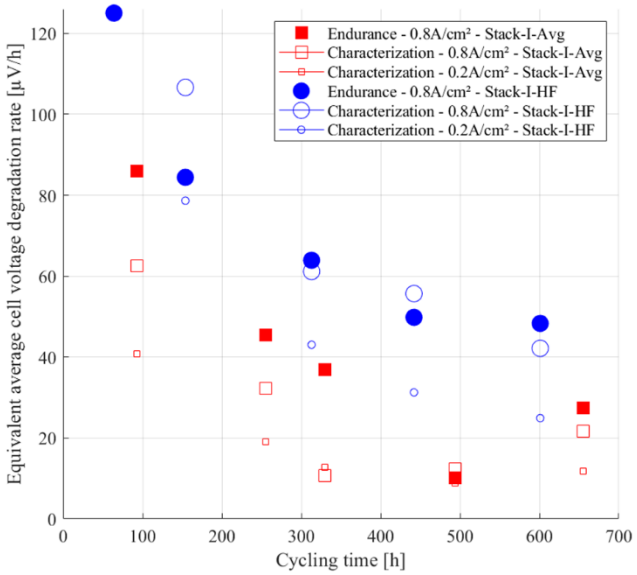

Fig. 6: Voltage degradation rate of the two stacks as a function of cycling time.

Fig. 6 shows the evolution of degradation rates calculated from polarization curves for the two current densities 0.2 and 0.8 A.cm^{-2} as a function of cycling time (time actually spent at constant current or with current harmonics). It also shows the evolution of endurance degradation rates calculated from the instantaneous stack voltage evolution. These rates correspond to the difference between the initial stack voltage and the voltage just before the shutdown preceding a given characterization, divided by the cycling time up to that characterization.

For both aging tests, the evolution of degradation rates calculated by the two methods (endurance and characterization) remains consistent. However, we note that throughout the test with current harmonics, the degradation rates are much higher than those obtained with the constant current test. Fig. 6 also shows that the gains linked to the recovery of reversible losses are greater for the *Stack-I-Avg* than for the *Stack-I-HF* over the first 600 hours of cycling. Indeed, the differences between endurance degradation rates at 0.8 A.cm^{-2} and those obtained from polarization curves at 0.8 A.cm^{-2} are much greater for the *Stack-I-Avg* than for the *Stack-I-HF*.

V. Conclusion

Aging tests were carried out on two LT-PEMFC stacks, under current ripples and at constant current. The results show that current ripples have a less marked impact on degradation rates calculated from the instantaneous voltage drop between two successive characterizations, except for the first 100 hours of testing. However, the degradation rates calculated from the instantaneous voltage considered throughout the aging test, and without taking into account the characterization phases, are higher for the test with current harmonics. This conclusion is also confirmed by the analysis of degradation rates derived from polarization curves. Stack aging is more pronounced under current harmonics. This study also shows the strong impact of current harmonics on the increase in internal leakage observed on the stack in question. It should be remembered that this study was carried out on prototypes from a previous generation of stacks. New aging tests investigating new frequency values and current ripple amplitudes are planned as part of this work with this same generation of stacks, but also with new-generation prototypes. Water management strategies could be tested in future aging tests, such as pulsed H_2 purges with high flow rates to facilitate water removal. Future results will play a crucial role in confirming the above findings.

Acknowledgements

The HEMOWHY project has benefited from a French government grant, managed by the Agence Nationale de la Recherche (ANR), under the future investment program integrated into France 2030, reference ANR-10-AIRT-01. We would like to thank the industrial members of the project: Airbus, Flying Whales, Liebherr Aerospace, Aerostack GmbH. We would also like to thank Alstom Hydrogène, not a partner in the HEMOWHY project, for supplying us with prototype stacks and beyond.

References

[1] J. Kurtz, S. Sprik, G. Saur, and S. Onorato, *Fuel Cell Electric Vehicle Durability and Fuel Cell Performance*, 2019. [Online]. Available: https://doi.org/NREL/TP-5400-73011

[2] U.S. Department of Energy, *2019 Annual Progress Report: DOE Hydrogen and Fuel Cells Program*, 2020. [Online]. Available: https://doi.org/DOE/GO-102020-5257

[3] N. Garland, T. Benjamin, and J. Kopasz, "DOE Fuel Cell Program: Durability Technical Targets and Testing Protocols," *ECS Trans.*, vol. 11, 2007. [Online]. Available: https://doi.org/10.1149/1.2781004

[4] Z. Yang, Q. Du, Z. Jia, et al., "A comprehensive proton exchange membrane fuel cell system model integrating various auxiliary subsystems," *Appl. Energy*, vol. 256, p. 113959, 2019.

[5] Z. Yang, Q. Du, Z. Jia, et al., "Effects of operating conditions on water and heat management by a transient multi-dimensional PEMFC system model," *Energy*, vol. 183, pp. 462–476, 2019.

[6] C. Bao, M. Ouyang, and B. Yi, "Modeling and control of air stream and hydrogen flow with recirculation in a PEM fuel cell system—I. Control-oriented modeling," *Int. J. Hydrogen Energy*, vol. 31, no. 13, pp. 1879–1896, 2006.

[7] C. Bao, M. Ouyang, and B. Yi, "Modeling and control of air stream and hydrogen flow with recirculation in a PEM fuel cell system—II. Linear and adaptive nonlinear control," *Int. J. Hydrogen Energy*, vol. 31, no. 13, pp. 1897–1913, 2006.

[8] D. Guilbert, A. Gaillard, A. Mohammadi, et al., "Investigation of the interactions between proton exchange membrane fuel cell and interleaved DC/DC boost converter in case of power switch faults," *Int. J. Hydrogen Energy*, vol. 40, no. 1, pp. 519–537, 2015.

[9] G. Fontes, C. Turpin, S. Astier, et al., "Interactions between fuel cells and power converters: Influence of current harmonics on a fuel cell stack," *IEEE Trans. Power Electron.*, vol. 22, no. 2, pp. 670–678, 2007.

[10] G. Fontès, *Modélisation et caractérisation de la pile PEM pour l'étude des interactions avec les convertisseurs statiques*, Ph.D, Inst. Nat. Polytech. Toulouse-INPT, 2005.

[11] J. Kim, M. Jang, B. Cho *et al.*, "Characteristic analysis and modeling on PEMFC degradation associated with low frequency ripple current effects," in *Proc. IEEE Energy Convers. Congr. Expo. (ECCE)*, 2011, pp. 3336–3342.
[12] B. Wahdame et al., "Impact of power converter current ripple on the durability of a fuel cell stack," in *Proc. 2008 IEEE Int. Symp. Ind. Electron.*, Cambridge, UK, Jun. 2008, pp. 1495–1500.
[13] M. Gerard, *Étude des interactions pile/système en vue de l'optimisation d'un générateur pile à combustible: interactions cœur de pile/compresseur et cœur de pile/convertisseur*, Ph.D, Liten, 2011.
[14] O. Rallières, *Modélisation et caractérisation de Piles A Combustible et Electrolyseurs PEM*, Ph.D., Inst. Nat. Polytech. Toulouse-INPT, 2011.
[15] T. Jarry, A. Jaafar, C. Turpin, et al., "Impact of high frequency current ripples on the degradation of high-temperature PEM fuel cells (HT-PEMFC)," *Int. J. Hydrogen Energy*, vol. 48, no. 54, pp. 20734–20742, 2023.
[16] Q. Li, Y. Huangfu, L. Xu, et al., "An improved floating interleaved boost converter with the zero-ripple input current for fuel cell applications," *IEEE Trans. Energy Convers.*, vol. 34, no. 4, pp. 2168–2179, 2019.
[17] S. K. Mazumder, R. K. Burra, and K. Acharya, "A ripple-mitigating and energy-efficient fuel cell power-conditioning system," *IEEE Trans. Power Electron.*, vol. 22, no. 4, pp. 1437–1452, 2007.
[18] Y. Zhan, Y. Guo, J. Zhu, et al., "A review on mitigation technologies of low frequency current ripple injected into fuel cell and a case study," *Int. J. Hydrogen Energy*, vol. 45, no. 46, pp. 25167–25190, 2020.
[19] G. Tsotridis, A. Pilenga, G. De Marco, et al., *EU harmonised test protocols for PEMFC MEA testing in single cell configuration for automotive applications*, Luxembourg: Publications Office of the European Union, 2015.
[20] J. Wu, X. Z. Yuan, H. Wang, et al., "Diagnostic tools in PEM fuel cell research: Part I Electrochemical techniques," *Int. J. Hydrogen Energy*, vol. 33, no. 6, pp. 1735–1746, 2008.
[21] S. M. R. Niya and M. Hoorfar, "Study of proton exchange membrane fuel cells using electrochemical impedance spectroscopy technique–A review," *J. Power Sources*, vol. 240, pp. 281–293, 2013.
[22] Z. Hua, Z. Zheng, E. Pahon, et al., "A review on lifetime prediction of proton exchange membrane fuel cells system," *J. Power Sources*, vol. 529, p. 231256, 2022.
[23] L. Vichard, F. Harel, A. Ravey, et al., "Degradation prediction of PEM fuel cell based on artificial intelligence," *Int. J. Hydrogen Energy*, vol. 45, no. 29, pp. 14953–14963, 2020.
[24] K. Chen, S. Laghrouche, and A. Djerdir, "Health state prognostic of fuel cell based on wavelet neural network and cuckoo search algorithm," *ISA Trans.*, vol. 113, pp. 175–184, 2021.
[25] K. Chen, S. Laghrouche, and A. Djerdir, "Aging prognosis model of proton exchange membrane fuel cell in different operating conditions," *Int. J. Hydrogen Energy*, vol. 45, no. 20, pp. 11761–11772, 2020.
[26] M. Jouin, R. Gouriveau, D. Hissel, et al., "Degradations analysis and aging modeling for health assessment and prognostics of PEMFC," *Rel. Eng. Syst. Saf.*, vol. 148, pp. 78–95, 2016.
[27] M. Jouin, R. Gouriveau, D. Hissel, et al., "Prognostics and Health Management of PEMFC–State of the art and remaining challenges," *Int. J. Hydrogen Energy*, vol. 38, no. 35, pp. 15307–15317, 2013.
[28] C. Robin, M. Gérard, M. Quinaud, et al., "Proton exchange membrane fuel cell model for aging predictions: Simulated equivalent active surface area loss and comparisons with durability tests," *J. Power Sources*, vol. 326, pp. 417–427, 2016.
[29] M. Jouin, R. Gouriveau, D. Hissel, et al., "Prognostics of PEM fuel cell in a particle filtering framework," *Int. J. Hydrogen Energy*, vol. 39, no. 1, pp. 481–494, 2014.
[30] R. Ma et al., "A Hybrid Prognostic Method for PEMFC with Aging Parameter Prediction," *IEEE Trans. Transp. Electrification*, pp. 1–1, 2021.
[31] M. Yue, Z. Li, R. Roche, et al., "Degradation identification and prognostics of proton exchange membrane fuel cell under dynamic load," *Control Eng. Pract.*, vol. 118, p. 104959, 2022.
[32] L. Zhu and J. Chen, "Prognostics of PEM fuel cells based on Gaussian process state space models," *Energy*, vol. 149, pp. 63–73, 2018.
[33] V. Phlippoteau, *Outils et Méthodes pour le diagnostic d'un état de santé d'une pile à combustible*, Ph.D., Inst. Nat. Polytech. Toulouse-INPT, 2009.